

000 001 002 003 004 Markovian Transformers for Informative Language Mod- eling

005 Anonymous authors
006 Paper under double-blind review

009 Abstract 010 011

012 Chain-of-Thought (CoT) reasoning often fails to faithfully reflect a lan-
013 guage model’s underlying decision process. We address this by introducing
014 a Markovian language model framework with an autoencoder-style reason-
015 ing bottleneck: it creates a text-based bottleneck where CoT serves as an
016 intermediate representation, forcing the model to compress essential rea-
017 soning into interpretable text before making predictions, in the sense of
018 learning short intermediate descriptions that make answers easy to com-
019 pute from questions. We train this system with a GRPO-style policy gradi-
020 ent algorithm using parallel sampling, a frozen baseline CoT’, within-batch
021 standardized advantages, and actor-reward (chain-rule) gradients. On QA
022 tasks, Markovian training recovers most of the gains of a non-Markovian
023 GRPO variant while forcing the model to answer from the CoT alone (e.g.,
024 GSM8K: 19.6% → 57.1%; ARC-Challenge: 36.1% → 79.9%; on average
025 only ≈3–4 pp below a non-Markovian upper bound). Perturbation analy-
026 ses across types and severities show that Markovian models incur system-
027 matically larger log-probability drops under CoT corruption than matched
028 Non-Markovian baselines, indicating stronger causal reliance on the CoT.
029 Cross-model evaluation confirms that learned CoTs generalize across ar-
030 chitectures, suggesting they capture transferable reasoning patterns rather
031 than model-specific artifacts.

032 1 Introduction 033

034
035 The rapid advancement of language models (LMs) has led to impressive performance on
036 complex cognitive tasks (Brown et al., 2020). Yet it is often unclear why an LM arrives at
037 a particular conclusion (Lamparth & Reuel, 2023; Burns et al., 2023; Gurnee & Tegmark,
038 2024), causing issues in high-stakes applications (Grabb et al., 2024; Lamparth et al., 2024;
039 Rivera et al., 2024). Traditional interpretability methods analyze hidden activations or
040 attention patterns to extract “explanations” (Geiger et al., 2022; Geva et al., 2022; Meng
041 et al., 2022; Casper et al., 2023; Wang et al., 2022; Lamparth & Reuel, 2023; Nanda et al.,
042 2023). Modern LMs, however, already generate coherent text: we might hope prompting
043 the model to articulate its reasoning (“Chain-of-Thought” or CoT) (Nye et al., 2022; Wei
044 et al., 2022) would yield a faithful record of its thought process.

045 Unfortunately, CoT explanations can be unfaithful. For example, Turpin et al. (2023) show
046 that spurious in-context biases often remain hidden in the CoT, and Lanham et al. (2023)
047 find that altering CoT text may not affect the final answer. Such observations indicate that
048 standard CoTs are not “load-bearing.”

049 In this work, we take a pragmatic approach to interpretability, focusing on informativeness
050 over full faithfulness. Rather than insisting the CoT mirrors the model’s entire internal
051 process, we require that the CoT alone suffices to produce the final answer. In other words,
052 if we remove the original prompt and rely only on the CoT, the model should still reach the
053 correct output. This makes the CoT causally essential and fragile: changing it necessarily
alters the prediction.

054 What distinguishes our approach is the clear distinction between the model relying on its
 055 CoT versus generating more informative CoTs. While traditional approaches train models
 056 to generate better-quality CoTs, they don't fundamentally change how the model uses them.
 057 Our Markovian framework, by contrast, forces the model to process information through
 058 the CoT bottleneck, making the CoT not just informative but causally load-bearing for
 059 prediction.

060 For instance, Llama's CoT on arithmetic tasks changed dramatically after training. Before
 061 training, it simply listed all numbers and their (incorrect) sum (e.g., "Sum = $76 + 90 + 92 +$
 062 ... = 2314"). After training, it performed correct step-by-step calculations (e.g., "calculate
 063 $6 + 89 = 95$; Next, calculate $95 + 38 = 133$..."), breaking the task into manageable steps
 064 that can be verified independently and enabling accurate answer prediction even when the
 065 original question is removed.

066 Recipient-Specific Compression. A key insight is that an informative CoT can also serve
 067 as a recipient-specific explanation or compression of the model's hidden knowledge: it dis-
 068 tills the essential reasoning into text that another recipient (e.g. a different model or a
 069 human) can use to predict the same outcome. Our experiments confirm that the learned
 070 CoTs generalize across interpreters, suggesting that these textual explanations genuinely
 071 encode transferable problem-solving steps rather than model-specific quirks (Section 5.4)
 072 and aligning with the explanation-theoretic view formalized in Section 3.4.
 073

074 Algorithmic view of explanations. Informally, we treat a CoT B for a question–answer pair
 075 (A, C) as a candidate explanation: a "good" explanation is a short intermediate description
 076 that makes the correct answer easy to compute from the question. In Section 3.4 we formalize
 077 this idea using a Levin-style resource-bounded complexity objective (?), and show that
 078 our Markovian design can be viewed as searching, within a bounded CoT space, for such
 079 explanations.

080 Contributions.

- 081
- 082 We introduce a Markovian language model framework that structurally enforces
 083 CoT generation to be causally essential, together with a GRPO-style training recipe
 084 (parallel sampling, frozen CoT baseline, actor-reward gradients) that optimizes this
 085 objective through a discrete text bottleneck.
 - 086 We apply this framework to arithmetic problems (Mistral 7B) and standard QA
 087 datasets (GSM8K, MMLU, SVAMP, ARC-Challenge; Llama 3.1 8B), observing
 088 large absolute gains over the base model (e.g., GSM8K 19.6% → 57.1%, ARC-
 089 Challenge 36.1% → 79.9%) while remaining within ≈3–4 percentage points of a Non-
 090 Markovian GRPO variant that can still see the question during answer prediction.
 - 091 We show through systematic perturbation analyses on Wikipedia continuation and
 092 multiple QA datasets that Markovian training produces consistently higher sensitiv-
 093 ity to CoT perturbations compared to matched Non-Markovian baselines (Tables 1
 094 and 3), indicating that the learned CoTs are more causally load-bearing.
 - 095 We demonstrate cross-model transfer: CoTs trained on one model (Llama 3.1 8B) re-
 096 main informative for diverse other models (Mistral, Phi, Qwen, GPT-2) on GSM8K
 097 and Wikipedia. This underscores the CoT's recipient-specific informativeness and
 098 suggests it captures a shared reasoning strategy rather than model-specific artifacts.

099 Section 2 reviews related work, Section 3 details our Markovian framework, and Section 4
 100 describes the RL training. Section 5 presents empirical results, and Section 6 discusses
 101 limitations and future directions.

103 2 Related Work

104 Prior work shows that CoT prompting can boost performance on reasoning tasks (Wei
 105 et al., 2022; Nye et al., 2022). Whereas typical CoT prompting methods do not alter a
 106 pre-trained model's parameters, some prior approaches do fine-tune the model for CoT

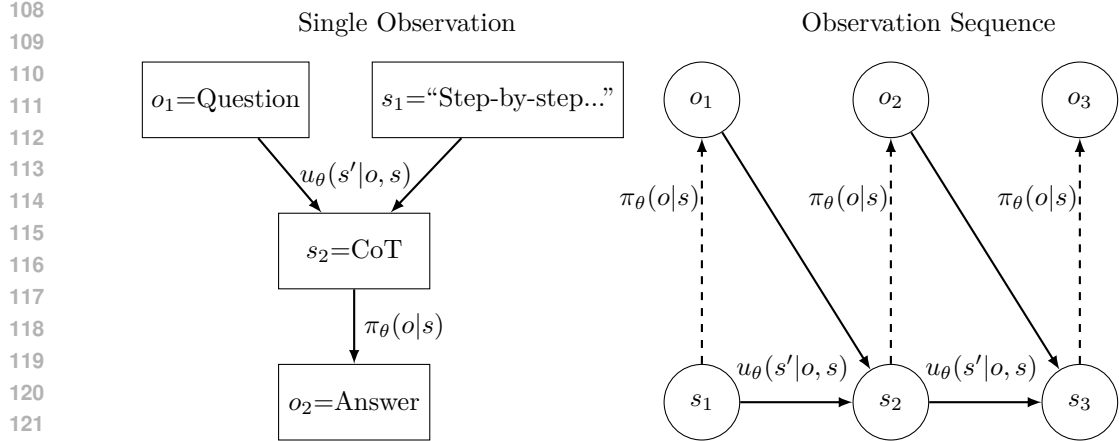


Figure 1: Markovian training as an autoencoder-style reasoning bottleneck. Left: Single time-step process from Question to CoT to Answer, creating a text-based bottleneck where the CoT must capture all information needed for answer prediction. Right: Causal structure showing the generation of states from observations and previous states using the state update function $u_\theta(s'|o, s)$, and the prediction of observations from states using the policy $\pi_\theta(o|s)$. This architecture forces reasoning through an interpretable text bottleneck, but prevents direct backpropagation, necessitating RL-based gradient estimation.

Dataset	Baseline	Non-Mkv	Mkv
GSM8K	19.6%	63.3%	57.1%
ARC-Chal	36.1%	78.6%	79.9%
Arithmetic	1.0%	97.0%	98.0%
MMLU	21.4%	68.7%	55.5%
SVAMP	18.0%	43.3%	42.3%

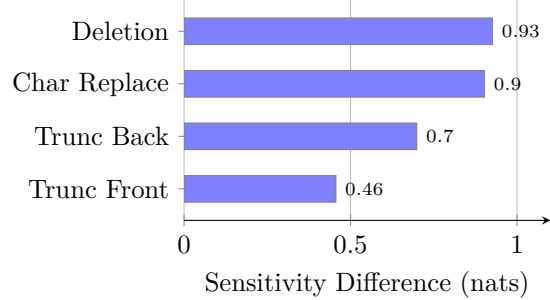


Figure 2: (a) Accuracy comparison. Markovian models (Mkv) maintain competitive performance with Non-Markovian upper bounds despite the strict information bottleneck. (b) Wiki perturbation sensitivity (positive = Mkv more fragile). Markovian models are significantly more sensitive to CoT corruption (higher $\Delta \ln P$), confirming the CoT is causally load-bearing.

generation (Zelikman et al., 2022; 2024; DeepSeek-AI et al., 2025). Our work differs by removing the original question or passage from the answer-prediction context, which enforces a stronger causal reliance on the CoT.

Regarding faithfulness vs. interpretability, some authors discuss how a CoT may fail to reflect the true reason the LM arrived at its answer (Lanham et al., 2023; Turpin et al., 2023), since small changes in the CoT do not necessarily change the final prediction. Zhou et al. (2023) analyze CoT through an information-theoretic lens, finding that CoT can serve as a communication channel between different parts of a model, ? use causal mediation analysis and a two-module training framework (FRODO) to measure and increase the causal effect of CoTs on answers, and ? highlight how preference optimization can lead to reward-hacking in explanations and propose using causal attributions to detect unfaithful CoTs. We build on these insights by training the model to rely on this channel exclusively.

Architecturally, our Markovian LM shares structural similarities with state space models like RNNs (Rumelhart et al., 1986), S4 (Gu et al., 2022), and Mamba (Gu & Dao, 2024), though with a key difference: MLMs have probabilistic state transitions to model token

sampling, which necessitates gradient estimation methods such as policy gradient (Sutton et al., 1999) rather than direct backpropagation. This probabilistic structure also resembles Kalman filters (Å ström, 1965), Deep Variational Bayes Filters (Karl et al., 2017), Deep Kalman Filters (Krishnan et al., 2015), and Variational Recurrent Neural Networks (VRNN) (Chung et al., 2015), though we use categorical rather than Gaussian distributions for interpretable text generation. Other fine-tuned reasoning models mentioned above (R1, STaR, and QuietSTaR) have similar structure but allow seeing the full context before generating state/reasoning tokens, whereas our approach enforces a strict information bottleneck through the state.

Lyu et al. (2023) also consider restricting the model’s ability to see the original input while generating the final answer. Their approach, however, involves rewriting the question in a structured formal language or code that is then executed. Our approach uses natural language for the reasoning state to preserve interpretability across diverse tasks.

3 Markovian Language Models and Informativeness

Here we provide our formalism for Markovian Language Models (MLMs) and define informativeness, which we use as a training objective within our novel structural framework.

3.1 Markovian Language Models (MLM)

A traditional LM can attend to the entire context when predicting the next token. This makes it possible for an LM to disregard the CoT or only partially rely on it. We impose a stricter, Markovian structure¹:

Definition 3.1 (Markovian LM). A Markovian Language Model is a tuple $M = (\mathcal{O}, \mathcal{S}, \pi, u, s_1)$, where

- \mathcal{O} is a set of observations (e.g., questions and answers in a QA task),
- \mathcal{S} is a set of states (e.g., CoT reasoning text),
- $\pi : \mathcal{S} \rightarrow \Delta(\mathcal{O})$ is a policy that predicts the next observation from the state alone,
- $u : \mathcal{O} \times \mathcal{S} \rightarrow \Delta(\mathcal{S})$ is a state update function (produces CoT from question and initial prompt),
- $s_1 \in \mathcal{S}$ is an initial state (starting CoT prompt).

For example, in a math reasoning task, $o_1 \in \mathcal{O}$ might be a question, $s_1 \in \mathcal{S}$ is an initial CoT prompt like “Let’s solve this step-by-step:”, $s_2 \in \mathcal{S}$ is the generated reasoning chain, and $o_2 \in \mathcal{O}$ is the answer. The key idea is that π can only see the CoT state s_2 when predicting o_2 , forcing the CoT to contain all needed information. Intuitively, π is the next-token predictor, and u chooses how to produce the CoT from the latest observation and prior state. In our experiments, π and u are the same underlying transformer; we denote the trainable pair by (u_θ, π_θ) and the frozen baseline pair by (u', π') .

3.2 Data-Generating Distribution and Reward

Let P be the distribution over observations $x_1, x_2, \dots, x_T \in \mathcal{O}$. A trajectory τ is generated by:

$$s_{t+1} \sim u_\theta(s_t, x_t), \quad x_{t+1} \sim P(x_{t+1} | x_{\leq t}),$$

with s_1 a fixed initial prompt. We define the reward for a trajectory τ as:

$$R_\theta(\tau) = \sum_{t=1}^T [\ln \pi_\theta(x_t | s_t) - \ln \pi'(x_t | s'_t)],$$

¹This structure can be viewed as a stochastic variant of a Moore machine where both the transition function (u) and output function (π) are probabilistic, and the input and output alphabets are identical (\mathcal{O}). Alternatively, an MLM can be formalized as an F-coalgebra where $F(S) = P(O) \times P(S)^O$, with P representing probability distributions.

216 where s'_t is generated by a baseline update function u' , e.g., the untrained model, and π' is
 217 the corresponding frozen baseline policy. In words, $R_\theta(\tau)$ measures how much more likely
 218 the correct observation x_t is under the trained state s_t (scored by π_θ) compared to the
 219 baseline state s'_t (scored by π').
 220

221 3.3 Informativeness Objective

223 Conceptually, we aim to ensure that the CoT state serves as a critical bottleneck for in-
 224 formation flow, making it causally essential for predictions. Formalizing this within our
 225 Markovian framework, we define:

$$226 J(\theta) = \mathbb{E}_{\tau \sim P, u_\theta, u'} [R_\theta(\tau)],$$

227 where θ parameterizes the trainable pair. Maximizing $J(\theta)$ ensures that the update function
 228 u_θ produces states s_t that are informative to π_θ about future observations (relative to the
 229 baseline u' and π'), thereby enforcing the CoT’s role as a load-bearing component. We
 230 optimize $J(\theta)$ with policy-gradient methods (including our GRPO-style update), sampling
 231 observations from P and states from u_θ and u' .

232 3.4 Explanation-Theoretic Objective

234 The informativeness objective $J(\theta)$ can also be understood through an explanation-theoretic
 235 lens that makes precise what we mean by a “good” CoT. Consider a question–answer or
 236 continuation instance, and write A for the input text (question or past context), C for the
 237 target text (answer or future continuation), and B for the CoT state produced by the update
 238 function u_θ .

239 Informally, following Levin’s notion of resource-bounded Kolmogorov complexity (?), an
 240 ideal explanation B for (A, C) should (i) make C easy to compute, (ii) be easy to compute
 241 from A , and (iii) be simple in its own right. We interpret our loss components in a minimum
 242 description length spirit: the negative log-probability $-\log \pi_\theta(C | B)$ plays the role of a
 243 description length for C given B , while using the frozen pre-trained model u' as a prior
 244 over CoTs makes $-\log u'(B | A)$ a description length for B given A . Together with the
 245 Markovian factorization $A \rightarrow B \rightarrow C$ and a hard length cap on B , this perspective suggests
 246 that training searches over short textual states B that serve as good explanations of C given
 247 A , without requiring B to be as complex as the full input (since irrelevant aspects of A can
 248 be dropped).

249 4 Methods

250 4.1 Implementation as Question-Answer Pairs

253 In many tasks like math problem solving, we have $T = 2$ observations (question and answer)
 254 and implement the abstract MLM with a fixed maximum length for the CoT state. Let \mathcal{V}
 255 be a token vocabulary. We set $\mathcal{O} = \mathcal{V}^N$ and $\mathcal{S} = \mathcal{V}^K$ for some $N, K \in \mathbb{N}$, where K is the
 256 maximum tokens in the CoT. Note that while we limit the state to a maximum of K tokens
 257 for implementation, we do not enforce fixed-length observations.

258 Our conceptual arguments rely on $K < N$, as otherwise the model could simply write the
 259 predicted observation into the state. We satisfy this in our Wikipedia experiments (Sec 5.2),
 260 and for other experiments we find empirically that the model does not learn this undesirable
 261 behavior due to the difficulty of predicting the answer directly without any CoT.

263 In this setting, we denote our states as $s_1 = \text{CoT}_{\text{init}}$ and $s_2 = \text{CoT}$, where CoT_{init} is a
 264 task-specific prompt². With pre-trained LM \mathcal{L} , we can implement our update function u
 265 and policy π using:

$$266 \ln u_\theta(s_2 = \text{CoT} | q, s_1 = \text{CoT}_{\text{init}}) = \sum_{i=1}^K \ln \mathcal{L}_\theta(\text{concat}(q, \text{CoT}_{\text{init}}, \text{CoT}_{<i}))[\text{CoT}_i],$$

269 ²The exact prompt template varies by task type, with each template specifying the task objective,
 allowed CoT length, and an invitation to reason strategically. Full templates are provided in Sec A.

$$\ln \pi_\theta(\text{ans} \mid \text{CoT}) := \sum_{i=1}^N \ln \mathcal{L}_\theta(\text{concat}(\text{CoT}, \text{ans}_{<i}))[\text{ans}_i].$$

Compression viewpoint. Throughout this work, when we speak of “CoT-as-compression” or simply “compression,” we refer not to the literal token length of the CoT, but to the resource-bounded description length of the future text or answer given the CoT. In continuation tasks (e.g., Wikipedia), the content to be predicted can be much longer than the CoT, so the CoT acts as a lossy compression of the future context in this MDL sense. In QA tasks, the answer string is typically shorter than the CoT, but the computational problem “which answer is correct?” can still have high resource-bounded complexity in the sense of Levin. Our Markovian constraint forces every prediction to factor as

$$A \rightarrow B \rightarrow C,$$

where B is a bounded-length CoT state. From the explanation-theoretic perspective of Section 3.4, the model is trained to find intermediate states B that make the answer easy to predict while discarding irrelevant information in A , so a good CoT can remain much simpler than the raw input even when the prompt is long.

Crucially, we do not allow the answer generation to attend back to the question q directly; the question is replaced by the CoT. For each question q , we generate the baseline state s'_2 (which we denote as CoT' in this setting) by prompting the unmodified pre-trained model u' with q plus an initial instruction (e.g., Think step-by-step...), and recording its raw output.

Our reward is:

$$R_\theta = \ln \pi_\theta(\text{ans} \mid \text{CoT}) - \ln \pi'(\text{ans} \mid \text{CoT}').$$

4.2 Policy Gradient with GRPO-Style Baseline

Markovian training can be viewed as the autoencoder-style reasoning bottleneck introduced in Section 3, where the CoT is a discrete text bottleneck between question and answer. This bottleneck blocks direct backpropagation through token sampling, so we rely on reinforcement learning techniques for gradient estimation.

4.2.1 Actor Reward Gradients: An Important Innovation

Our approach differs from standard policy gradient setups, where the reward $R(\tau)$ is treated as independent of the policy parameters (or any θ -dependence is stopped by gradient detachment). Here the same transformer with weights θ defines both the sampling distribution $P_\theta(\tau)$ via u_θ and the reward term $\ln \pi_\theta(\text{ans} \mid \text{CoT})$, and we explicitly backpropagate through this reward in addition to the usual REINFORCE term.

However, in our case, the reward is a function of the same parameters via the actor term: $R_\theta(\tau) = \ln \pi_\theta(\text{ans} \mid \text{CoT}) - \ln \pi'(\text{ans} \mid \text{CoT}')$. Applying the chain rule:

$$\nabla_\theta \mathbb{E}_{\tau \sim P_\theta}[R_\theta(\tau)] = \mathbb{E}_{\tau \sim P_\theta}[R_\theta(\tau) \nabla_\theta \ln P_\theta(\tau) + \nabla_\theta R_\theta(\tau)].$$

This yields two terms: the standard policy gradient ($R_\theta(\tau) \cdot \nabla_\theta \ln P_\theta(\tau)$) and the direct reward gradient ($\nabla_\theta R_\theta(\tau)$). We include both terms with equal weight in our implementation.

4.2.2 GRPO-Style Baseline with Local Subtraction

We implement a policy gradient algorithm inspired by Group Relative Policy Optimization (GRPO), originally introduced by Shao et al. Shao et al. (2024) in DeepSeek-Math, which eliminates the critic model from PPO by using group-based advantage estimation where multiple responses to the same query provide relative baselines for each other. We add an additional baseline subtraction step before applying GRPO’s batch averaging: we first compute a local baseline using the frozen reference model u' , then apply GRPO-style standardization within each batch.

324 Algorithm 1 Markovian Training with GRPO-Style Batch Baseline
 325
 326 1: Given dataset P of (q, a) , trainable actor (u_θ, π_θ) , frozen baseline (u', π') , batch size B
 327 2: for each training batch do
 328 3: Sample $(q, a) \sim P$
 329 4: Sample $\text{CoT}_i \sim u_\theta(\cdot | q, \text{CoT}_{\text{init}})$ for $i = 1..B$ (stochastic parallel sampling)
 330 5: Sample baseline $\text{CoT}' \sim u'(\cdot | q, \text{CoT}_{\text{init}})$ (once per batch)
 331 6: Compute actor answer log-probs $r_i = \ln \pi_\theta(a | \text{CoT}_i)$
 332 7: Compute baseline log-prob $b = \ln \pi'(a | \text{CoT}')$
 333 8: Normalized rewards $R_i = r_i - b$; standardize within-batch: $A_i = \frac{R_i - \mu}{\sigma + \epsilon}$
 334 9: Policy gradient loss: $\ell_i^{\text{PG}} = -\ln u_\theta(\text{CoT}_i | q, \text{CoT}_{\text{init}}) \cdot A_i^{\text{detach}}$
 335 10: Actor-reward gradient: $\ell_i^{\text{AR}} = -A_i$
 336 11: KL penalty: $\ell_i^{\text{KL}} = 0.1 D_{KL}(u_\theta(\cdot | q) \| u'(\cdot | q))$
 337 12: Total loss: $\ell_i = \ell_i^{\text{PG}} + \ell_i^{\text{AR}} + \ell_i^{\text{KL}}$; update θ with $\frac{1}{B} \sum_i \ell_i$
 338 13: end for
 339
 340

4.2.3 Parallel Sampling Strategy

We employ parallel sampling (inspired by GRPO): each training batch contains B copies of the same question-answer pair (q, a) , and the trainable model u_θ generates diverse reasoning chains $\{\text{CoT}_1, \text{CoT}_2, \dots, \text{CoT}_B\}$ for the identical input through stochastic sampling. Additionally, a frozen baseline model u' generates a single reference CoT' per batch that provides a local baseline before applying GRPO-style batch averaging.

4.2.4 Implementation: Two-Term Loss Function

Our implementation combines both gradient terms from the chain rule derivation above. The loss function includes:

$$\mathcal{L} = \mathcal{L}_{\text{PG}} + \mathcal{L}_{\text{AR}}, \quad \mathcal{L}_{\text{PG}} = -\ln u_\theta(\text{CoT} | q, \text{CoT}_{\text{init}}) \cdot A^{\text{detach}}, \quad \mathcal{L}_{\text{AR}} = -A.$$

where A is the standardized advantage (after local baseline subtraction and GRPO-style batch averaging) and A^{detach} blocks gradients to isolate the policy gradient term, enabling simultaneous optimization of CoT generation (via \mathcal{L}_{PG}) and answer prediction (via \mathcal{L}_{AR}).

4.2.5 Within-Batch Advantage Standardization

Instead of historical exponential moving averages, we standardize advantages within each batch so that they have zero mean and unit variance (Algorithm 1), which stabilizes training regardless of the absolute reward scale.

From a coding-theoretic perspective, $-\log u'(B | q)$ is the description length of a CoT B under the frozen model's prior, so the KL term acts as a computable surrogate for penalizing complex or idiosyncratic explanations B , while the answer log-probability $\log \pi_\theta(a | B)$ rewards CoTs that make a easy to predict (cf. the explanation-theoretic discussion in Section 3.4).

5 Experiments

We evaluate in two regimes: (i) continuation (Wikipedia), where CoT tokens act as a short explanatory state summarizing longer context (our “CoT-as-compression” view), and (ii) question-answer datasets (GSM8K, MMLU, SVAMP, ARC, Arithmetic), which validate the general-purpose efficacy of Markovian training even when raw token lengths alone do not capture the compression story.

5.1 Question–Answer Tasks (GSM8K, MMLU, SVAMP, ARC, Arithmetic)

We evaluate on standard QA-style datasets (GSM8K (Cobbe et al., 2021), MMLU (Hendrycks et al., 2020), SVAMP (Patel et al., 2021), ARC Challenge (Clark et al.,

378
 379
 380
 381
 382
 383
 384
 385
 386
 387
 388
 389
 390
 391
 392
 393
 394
 395
 396
 397
 398
 399
 400
 401
 402
 403
 404
 405
 406
 407
 408
 409
 410
 411
 412
 413
 414
 415
 416
 417
 418
 419
 420
 421
 422
 423
 424
 425
 426
 427
 428
 429
 430
 431
 2018), and our non-standard multi-step addition task. All QA experiments use the same optimization: GRPO-style parallel sampling with within-batch standardization and the chain-rule reward (policy-gradient plus actor-reward gradient), with task-specific default CoT lengths. For arithmetic, each problem has fifteen random terms in [1, 99]; the model learns to produce step-wise reasoning and achieves > 99% verbatim-correct answers at $T=0$.

CoT length defaults. Unless otherwise specified, we use: GSM8K 100, Arithmetic 150, MMLU 150, SVAMP 50, and ARC-Challenge 50. See §4 for objective details.

5.2 Wikipedia Continuation

For Wikipedia continuation (Foundation, 2024), we condition on the first 200 tokens and predict the next 100 tokens, allowing 50 tokens of CoT. Training uses the same GRPO with chain-rule reward as in QA. We observe improvements consistent with increased CoT informativeness (cf. Fig. 2), and §5.3 shows stronger perturbation sensitivity under Markovian training.

Severity	Char Replace	Delete	Digit Replace	Truncate Back	Truncate Front	Row Mean
20%	+0.457	+0.459	+0.016	+0.254	-0.009	+0.235
40%	+0.849	+0.836	+0.025	+0.368	+0.121	+0.440
60%	+1.042	+1.002	+0.035	+0.596	+0.284	+0.592
80%	+1.079	+1.069	+0.038	+1.020	+0.622	+0.766
100%	+1.084	+1.263	+0.039	+1.258	+1.262	+0.981
Column Mean	+0.902	+0.926	+0.030	+0.699	+0.456	+0.603

Table 1: Perturbation fragility on Wikipedia continuation. Entries report $\Delta \ln P = (\text{Markovian drop} - \text{Non-Markovian drop})$, where the Markovian drop is $\ln \pi_\theta(\text{ans} | \text{CoT}^M) - \ln \pi_\theta(\text{ans} | \widetilde{\text{CoT}}^M)$ and the Non-Markovian drop is $\ln \pi_{\theta'}(\text{ans} | q, \text{CoT}^{NM}) - \ln \pi_{\theta'}(\text{ans} | q, \widetilde{\text{CoT}}^{NM})$. Here θ denotes the Markovian checkpoint that must answer from the CoT alone, while θ' is the Non-Markovian checkpoint that additionally conditions on the question q . Values are averaged over 1,024 held-out examples per perturbation type and severity. Positive values mean the Markovian actor relies more on intact CoTs. Row means summarize severity-wise fragility, while the column-mean row highlights which perturbation families disrupt Markovian reasoning the most (delete and truncate operations produce the largest gaps).

5.3 Markovian vs Non-Markovian Perturbation Sensitivity

To provide systematic evidence for the theoretical advantages of Markovian training, we conduct comprehensive perturbation sensitivity comparisons between Markovian and Non-Markovian model pairs. The Non-Markovian models are trained using the same hyperparameters, only differing in that the reward is $\pi_{\theta'}(\text{ans} | q, \text{CoT})$ instead of $\pi_\theta(\text{ans} | \text{CoT})$. This analysis directly evaluates whether the structural constraints in Markovian training lead to measurably different robustness properties during training.

5.3.1 Experimental Design

We maintain two independently trained checkpoints: the Markovian weights θ , which are always asked to score ans conditioned solely on the actor’s CoT, and the Non-Markovian weights θ' , which additionally attend to the original question q during both training and evaluation. For each held-out (q, ans) pair we run both models on the same data point, sampling fresh reasoning traces $\text{CoT}^M \sim u_\theta(\cdot | q)$ and $\text{CoT}^{NM} \sim u_{\theta'}(\cdot | q)$. We then perturb each CoT independently, producing $\widetilde{\text{CoT}}^M$ and $\widetilde{\text{CoT}}^{NM}$, and ask the corresponding model (using its own weights and visibility constraints) to score the answer with the original versus perturbed CoT. This provides two drop measurements per example that are directly com-

parable because they originate from models trained under different structural assumptions but evaluated on the same underlying data.

We test four perturbation types at five severities (20%, 40%, 60%, 80%, 100%):

- Delete: Random token deletion from CoT reasoning
- Digit Replace: Random replacement of numeric characters within tokens
- Truncate Front: Removal of tokens from CoT beginning
- Truncate Back: Removal of tokens from CoT end
- Character Replace: Random character substitution within tokens

The sensitivity measure matches the implementation:

$$\text{Effect}_M = \ln \pi_\theta(\text{ans} | \text{CoT}^M) - \ln \pi_\theta(\text{ans} | \widetilde{\text{CoT}}^M) \quad (1)$$

$$\text{Effect}_{NM} = \ln \pi_{\theta'}(\text{ans} | q, \text{CoT}^{NM}) - \ln \pi_{\theta'}(\text{ans} | q, \widetilde{\text{CoT}}^{NM}) \quad (2)$$

$$\text{Difference} = \text{Effect}_M - \text{Effect}_{NM} \quad (3)$$

Positive differences indicate greater Markovian sensitivity to CoT perturbations, reflecting stronger reliance on CoT integrity.

5.3.2 Results Summary

Table 1 averages 1,024 examples per perturbation/severity bucket. The Markovian–Non-Markovian gap grows from +0.235 at 20% severity to +0.981 at 100%, with delete and character-replace perturbations showing the largest effects and all entries positive, confirming that Markovian checkpoints consistently incur larger probability drops under CoT corruption than their Non-Markovian counterparts.

5.4 Interpretability of CoT Generations

To probe how well the reasoning generalizes, we evaluated the informativeness of Llama’s trained CoTs with respect to various other language models on the GSM8K dataset, and observed strong correlation between improvements in the trained model’s evaluation of CoT quality and the evaluations of alternative models throughout training.

We test across three distinct model families (Phi (Abdin et al., 2024), Mistral, and GPT2), including GPT2, a significantly smaller model that should not be able to decode sophisticated steganography. The fact that trained CoTs transfer effectively across this diverse set (Figure 3) confirms they contain generalizable reasoning patterns rather than model-specific artifacts and, in both continuation and QA settings, act as load-bearing explanations in the sense of Section 3.4.

6 Discussion and Limitations

Experiments across arithmetic, GSM8K, and Wikipedia show that it is possible to learn informative and interpretable CoT reasoning via RL on an LM using Markovian training. In continuation settings, our use of log-probability improvements is grounded in the fundamental objective of language modeling (maximizing the expected log-probability of future text), so perturbation-induced drops provide a natural metric for how well the CoT captures essential information. Viewed through the explanation-theoretic lens of Section 3.4, our results suggest that Markovian training learns short intermediate states B that make the answer C easy to compute from the question A while remaining relatively simple themselves: the architecture enforces the factorization $A \rightarrow B \rightarrow C$ with a bounded-length CoT state, and the RL objective (answer log-probability relative to a frozen baseline plus a KL penalty on the CoT policy) serves as a computable surrogate for the idealized explanation functional without requiring B to scale in complexity with the full question.

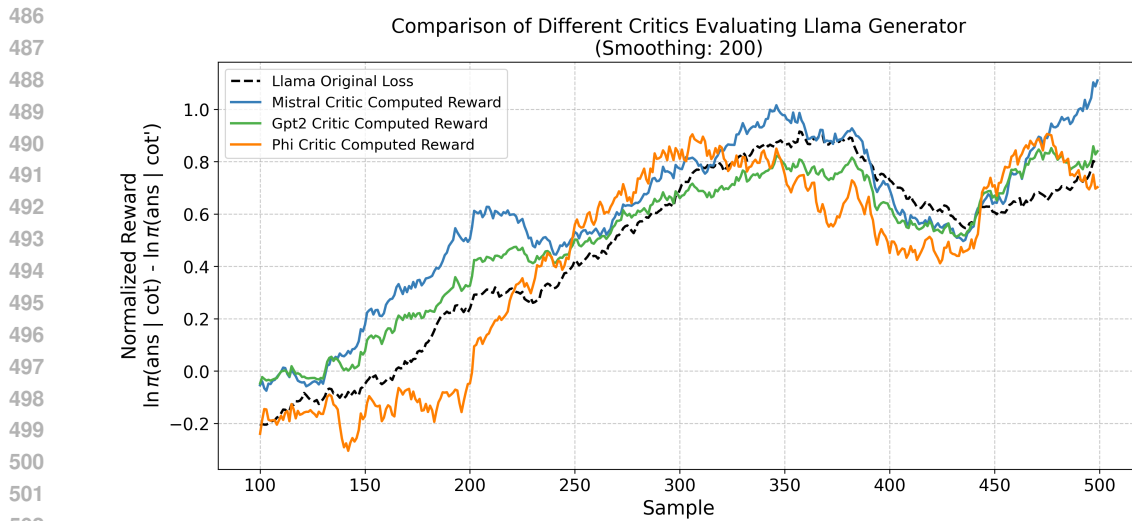


Figure 3: Cross-model evaluation comparing how different models (Mistral, GPT2, and Phi 3.5 Mini Instruct) utilize Llama 8B’s CoT on GSM8K. Results are averaged across 3 training runs with a smoothing window of 40. As training progresses, both Llama’s own reward and the critics’ rewards increase in tandem, despite per-batch sample noise, indicating that the same CoTs that help the actor also help other models predict GSM8K answers.

6.1 Algorithmic Ablations

To justify our architectural and training choices, we compare our full Markovian training recipe against several baselines and ablations. Table 2 summarizes the results across multiple datasets.

Table 2: Algorithmic ablations (Accuracy). Markovian uses our full GRPO-style training with actor-reward gradients. No Reward Grad removes the $\nabla_\theta R_\theta$ term. EI (Expert Iteration) replaces GRPO with rejection sampling. Non-Markovian allows the answer predictor to see the original question (an upper bound). Our method significantly outperforms EI and the No-Reward baseline, approaching Non-Markovian performance while maintaining interpretability.

Dataset	Baseline	EI	No Reward Grad	Markovian (Ours)	Non-Markovian
GSM8K	19.6%	61.6%	62.2%	57.1%	63.3%
ARC-Chal	36.1%	65.6%	79.3%	79.9%	78.6%
MMLU	21.4%	53.2%	46.6%	55.5%	68.7%
SVAMP	18.0%	38.7%	40.7%	42.3%	43.3%
Arithmetic	1.0%	76.0%	81.0%	98.0%	97.0%
Mean	19.2%	59.0%	61.9%	66.6%	70.2%

Algorithmic ablations. Parallel training with batch-standardized advantages (GRPO-style) consistently outperforms Expert Iteration (EI) and shows that actor-reward gradients matter: for example, on Arithmetic Markovian training achieves 98.0% versus EI’s 76.0%, and removing the chain-rule term ($\nabla_\theta R_\theta$) reduces performance from 98.0% to 81.0%. Similar trends hold on GSM8K, ARC-Challenge, MMLU, and SVAMP, where our full Markovian recipe approaches the Non-Markovian upper bound while preserving the interpretability benefits of the bottleneck.

We currently verify interpretability on myopic QA and continuation settings. A direct human study could further validate whether CoTs are genuinely human-interpretable beyond our model-centric proxies (fragility and cross-model transfer); we view these metrics as pragmatic but imperfect stand-ins for full faithfulness.

540 7 Reproducibility Statement
 541

542 We provide all source code, training and evaluation scripts, and detailed instructions in the
 543 README, including the main training loop (`src/train.py`) and analysis scripts for fragility
 544 and cross-model interpretability. Our implementation supports a range of public Hugging-
 545 Face models with LoRA fine-tuning (e.g., Llama 3.1 8B, Qwen3 4B, Mistral 7B, Phi 3.5,
 546 GPT-2, Gemma-3, TinyStories) and the full set of datasets used in this paper (arithmetic,
 547 GSM8K, MMLU, SVAMP, ARC-Challenge, and Wikipedia continuation). With these ma-
 548 terials, researchers should be able to reproduce our results, including the performance im-
 549 provements on GSM8K and the perturbation analyses demonstrating CoT reliance.

550
 551 References
 552

553 Karl Johan Å ström. Optimal control of markov processes with incomplete state information
 554 i, 1965.

555 Marah Abdin, Jyoti Aneja, Hany Awadalla, Ahmed Awadallah, Ammar Ahmad Awan,
 556 Nguyen Bach, Amit Bahree, Arash Bakhtiari, Jianmin Bao, et al. Phi-3 technical report:
 557 A highly capable language model locally on your phone, 2024.

559 Yuntao Bai, Saurav Kadavath, Sandipan Kundu, Amanda Askell, Jackson Kernion, Andy
 560 Jones, Anna Chen, Anna Goldie, Azalia Mirhoseini, Cameron McKinnon, Carol Chen,
 561 Catherine Olsson, Christopher Olah, Danny Hernandez, Dawn Drain, Deep Ganguli,
 562 Dustin Li, Eli Tran-Johnson, Ethan Perez, Jamie Kerr, Jared Mueller, Jeffrey Ladish,
 563 Joshua Landau, Kamal Ndousse, Kamile Lukosuite, Liane Lovitt, Michael Sellitto, Nel-
 564 son Elhage, Nicholas Schiefer, Noemi Mercado, Nova DasSarma, Robert Lasenby, Robin
 565 Larson, Sam Ringer, Scott Johnston, Shauna Kravec, Sheer El Showk, Stanislav Fort,
 566 Tamera Lanham, Timothy Telleen-Lawton, Tom Conerly, Tom Henighan, Tristan Hume,
 567 Samuel R. Bowman, Zac Hatfield-Dodds, Ben Mann, Dario Amodei, Nicholas Joseph,
 568 Sam McCandlish, Tom Brown, and Jared Kaplan. Constitutional ai: Harmlessness from
 569 ai feedback, 2022.

570 Tom Brown, Benjamin Mann, Nick Ryder, Melanie Subbiah, Jared D Kaplan, Prafulla
 571 Dhariwal, et al. Language models are few-shot learners, 2020.

572 Collin Burns, Haotian Ye, Dan Klein, and Jacob Steinhardt. Discovering latent knowledge
 573 in language models without supervision, 2023.

575 Stephen Casper, Tilman Rauker, Anson Ho, and Dylan Hadfield-Menell. Sok: Toward
 576 transparent ai: A survey on interpreting the inner structures of deep neural networks,
 577 2023.

578 Lili Chen, Kevin Lu, Aravind Rajeswaran, Kimin Lee, Aditya Grover, Michael Laskin,
 579 Pieter Abbeel, Aravind Srinivas, and Igor Mordatch. Decision transformer: Reinforcement
 580 learning via sequence modeling. In Advances in Neural Information Processing Systems,
 581 2021.

583 Paul Christiano, Ajeya Cotra, and Mark Xu. Eliciting latent knowledge: How to tell if your
 584 eyes deceive you, 2021.

585 Paul Christiano, Jan Leike, Tom B. Brown, Miljan Martic, Shane Legg, and Dario Amodei.
 586 Deep reinforcement learning from human preferences, 2023.

588 Junyoung Chung, Kyle Kastner, Laurent Dinh, Kratarth Goel, Aaron C. Courville, and
 589 Yoshua Bengio. A recurrent latent variable model for sequential data, 2015.

591 Peter Clark, Isaac Cowhey, Oren Etzioni, Tushar Khot, Ashish Sabharwal, Carissa
 592 Schoenick, and Oyvind Tafjord. Think you have solved question answering? try arc,
 593 the ai2 reasoning challenge. In Proceedings of the 2018 Workshop on Machine Reading
 594 for Question Answering, 2018.

- 594 Karl Cobbe, Vineet Kosaraju, Mohammad Bavarian, Mark Chen, Heewoo Jun, Lukasz
 595 Kaiser, Matthias Plappert, Jerry Tworek, Jacob Hilton, Reiichiro Nakano, Christopher
 596 Hesse, and John Schulman. Training verifiers to solve math word problems, 2021.
 597
- 598 DeepSeek-AI, Daya Guo, Dejian Yang, Haowei Zhang, Junxiao Song, Ruoyu Zhang, Runxin
 599 Xu, et al. Deepseek-r1: Incentivizing reasoning capability in llms via reinforcement learn-
 600 ing, 2025.
- 601 Wikimedia Foundation. Wikipedia, 2024.
 602
- 603 Atticus Geiger, Zhengxuan Wu, Hanson Lu, Josh Rozner, Elisa Kreiss, Thomas Icard, Noah
 604 Goodman, and Christopher Potts. Inducing causal structure for interpretable neural
 605 networks, 2022.
- 606 Mor Geva, Avi Caciularu, Kevin Ro Wang, and Yoav Goldberg. Transformer feed-forward
 607 layers build predictions by promoting concepts in the vocabulary space, 2022.
 608
- 609 Declan Grabb, Max Lamparth, and Nina Vasan. Risks from language models for automated
 610 mental healthcare: Ethics and structure for implementation, 2024.
- 611 Albert Gu and Tri Dao. Mamba: Linear-time sequence modeling with selective state spaces,
 612 2024.
 613
- 614 Albert Gu, Karan Goel, and Christopher Ré. Efficiently modeling long sequences with
 615 structured state spaces, 2022.
- 616 Wes Gurnee and Max Tegmark. Language models represent space and time, 2024.
 617
- 618 Dan Hendrycks, Collin Burns, Steven Basart, Andy Zou, Mantas Mazeika, Dawn Song, and
 619 Jacob Steinhardt. Measuring massive multitask language understanding. arXiv preprint
 620 arXiv:2009.03300, 2020.
- 621 Edward J Hu, Yelong Shen, Phillip Wallis, Zeyuan Allen-Zhu, Yuanzhi Li, Shean Wang,
 622 Lu Wang, and Weizhu Chen. Lora: Low-rank adaptation of large language models, 2022.
- 624 Nitish Joshi, Javier Rando, Abulhair Saparov, Najoung Kim, and He He. Personas as a way
 625 to model truthfulness in language models, 2024.
- 626 Maximilian Karl, Maximilian Soelch, Justin Bayer, and Patrick van der Smagt. Deep vari-
 627 ational bayes filters: Unsupervised learning of state space models from raw data, 2017.
- 629 Rahul G. Krishnan, Uri Shalit, and David Sontag. Deep kalman filters, 2015.
 630
- 631 Max Lamparth and Anka Reuel. Analyzing and editing inner mechanisms of backdoored
 632 language models, 2023.
- 633 Max Lamparth, Anthony Corso, Jacob Ganz, Oriana Skylar Mastro, Jacquelyn Schneider,
 634 and Harold Trinkunas. Human vs. machine: Language models and wargames, 2024.
 635
- 636 Tamera Lanham, Anna Chen, Ansh Radhakrishnan, Benoit Steiner, Carson Denison, Danny
 637 Hernandez, Dustin Li, Esin Durmus, Evan Hubinger, Jackson Kernion, Kamilé Lukošiūtė,
 638 Karina Nguyen, Newton Cheng, Nicholas Joseph, Nicholas Schiefer, Oliver Rausch, Robin
 639 Larson, Sam McCandlish, Sandipan Kundu, Saurav Kadavath, Shannon Yang, Thomas
 640 Henighan, Timothy Maxwell, Timothy Telleen-Lawton, Tristan Hume, Zac Hatfield-
 641 Dodds, Jared Kaplan, Jan Brauner, Samuel R. Bowman, and Ethan Perez. Measuring
 642 faithfulness in chain-of-thought reasoning, 2023.
- 643 Stephanie Lin, Jacob Hilton, and Owain Evans. Truthfulqa: Measuring how models mimic
 644 human falsehoods, 2022.
 645
- 646 Wang Ling, Dani Yogatama, Chris Dyer, and Phil Blunsom. Program induction by rationale
 647 generation: Learning to solve and explain algebraic word problems. In Proceedings of the
 55th Annual Meeting of the Association for Computational Linguistics (ACL), 2017.

- 648 Qing Lyu, Shreya Havaldar, Adam Stein, Li Zhang, Delip Rao, Eric Wong, Marianna Apid-
 649 ianaki, and Chris Callison-Burch. Faithful chain-of-thought reasoning, 2023.
 650
- 651 Kevin Meng, David Bau, Alex J Andonian, and Yonatan Belinkov. Locating and editing
 652 factual associations in gpt, 2022.
- 653 Neel Nanda, Lawrence Chan, Tom Lieberum, Jess Smith, and Jacob Steinhardt. Progress
 654 measures for grokking via mechanistic interpretability, 2023.
- 655 Maxwell Nye, Anders Johan Andreassen, Guy Gur-Ari, Henryk Michalewski, Jacob Austin,
 656 David Bieber, David Dohan, Aitor Lewkowycz, Maarten Bosma, David Luan, Charles
 657 Sutton, and Augustus Odena. Show your work: Scratchpads for intermediate computation
 658 with language models, 2022.
- 659
- 660 Prateek Patel, Satwik Bhattacharya, and Navin Goyal. Are nlp models really robust? a
 661 case study on numerical reasoning. In Proceedings of the 2021 Conference on Empirical
 662 Methods in Natural Language Processing, 2021.
- 663 Juan-Pablo Rivera, Gabriel Mukobi, Anka Reuel, Max Lamparth, Chandler Smith, and
 664 Jacquelyn Schneider. Escalation risks from language models in military and diplomatic
 665 decision-making, 2024.
- 666
- 667 David E. Rumelhart, Geoffrey E. Hinton, and Ronald J. Williams. Learning representations
 668 by back-propagating errors, 1986.
- 669 Zhihong Shao, Peiyi Wang, Qihao Zhu, Runxin Xu, Junxiao Song, Xiao Bi, Haowei Zhang,
 670 Mingchuan Zhang, Y.K. Li, Y. Wu, and Daya Guo. Deepseekmath: Pushing the limits of
 671 mathematical reasoning in open language models, 2024.
- 672
- 673 D. Silver, A. Huang, C. Maddison, et al. Mastering the game of go with deep neural networks
 674 and tree search, 2016.
- 675
- 676 David Silver, Thomas Hubert, Julian Schrittwieser, Ioannis Antonoglou, Matthew Lai,
 677 Arthur Guez, Marc Lanctot, Laurent Sifre, Dharshan Kumaran, Thore Graepel, Timothy
 678 Lillicrap, Karen Simonyan, and Demis Hassabis. Mastering chess and shogi by self-play
 679 with a general reinforcement learning algorithm, 2017.
- 680 Richard S. Sutton, David McAllester, Satinder Singh, and Yishay Mansour. Policy gradient
 681 methods for reinforcement learning with function approximation, 1999.
- 682
- 683 Katherine Tian, Eric Mitchell, Huaxiu Yao, Christopher D. Manning, and Chelsea Finn.
 Fine-tuning language models for factuality, 2023.
- 684 Miles Turpin, Julian Michael, Ethan Perez, and Samuel R. Bowman. Language models don't
 685 always say what they think: Unfaithful explanations in chain-of-thought prompting, 2023.
- 686
- 687 Kevin Ro Wang, Alexandre Variengien, Arthur Commy, Buck Shlegeris, and Jacob Stein-
 688 hardt. Interpretability in the wild: a circuit for indirect object identification in gpt-2
 689 small, 2022.
- 690 Jason Wei, Xuezhi Wang, Dale Schuurmans, Maarten Bosma, brian ichter, Fei Xia, Ed H.
 691 Chi, Quoc V Le, and Denny Zhou. Chain of thought prompting elicits reasoning in large
 692 language models, 2022.
- 693 Zichao Yang, Phil Blunsom, Chris Dyer, and Wang Ling. Reference-aware language models,
 694 2017.
- 695
- 696 Eric Zelikman, Yuhuai Wu, Jesse Mu, and Noah Goodman. Star: Bootstrapping reasoning
 697 with reasoning, 2022.
- 698
- 699 Eric Zelikman, Georges Harik, Yijia Shao, Varuna Jayasiri, Nick Haber, and Noah D. Good-
 700 man. Quiet-star: Language models can teach themselves to think before speaking, 2024.
- 701 Dani Zhou, Enyu Zhou, Kevin Han, and Prashant Kambadur. Understanding chain-of-
 thought in llms through information theory, 2023.

702 A Training Stability and Implementation Details 703

704 Fine-tuning a pre-trained language model with a strong linguistic prior requires careful
705 consideration to avoid irrecoverable weight updates that could push the model out of the
706 language modeling loss basin. We implement several techniques to enhance training stability
707 for the GRPO objective:

- 709 1. Low-Rank Adaptation (LoRA) (Hu et al., 2022):
 - 710 • Freeze all weights except for small-rank LoRA adapters.
 - 711 • Use rank 8 with $\alpha = 16$.
- 713 2. Gradient Clipping:
 - 714 • If the ℓ_2 norm of the gradient exceeds 1.0, rescale it to norm 1.0.
- 715 3. Within-Batch Advantage Standardization:
 - 716 • GRPO’s parallel sampling enables robust within-batch standardization, eliminating
717 the need for historical baselines.
 - 718 • Each batch provides its own reference distribution for advantage calculation.
- 720 4. Actor Reward Weight:
 - 721 • Set actor reward weight to 1.0 to equally balance policy gradient and direct
722 reward optimization.
 - 723 • This enables end-to-end learning through the reward model.
- 725 5. Initial CoT Prompt Design:
 - 726 • Choose CoT_{init} to guide the model toward meaningful reasoning.
 - 727 • For arithmetic:
728 “You will be given an arithmetic problem, which you have [CoT length] tokens
729 to work through step-by-step. Question:”
 - 730 • For GSM8K:
731 “You will be given a reasoning problem, which you have [CoT length] tokens
732 to work through step-by-step. Question:”
 - 733 • For Wikipedia continuation:
734 “Compress your understanding of this text into [CoT length] tokens, then
735 predict the next [target length] tokens.”

736 These measures greatly reduce the risk of catastrophic updates and keep the model’s training
737 on track.

739 B Extended Perturbation Analysis 740

742 This section provides a detailed breakdown of perturbation fragility across different datasets.
743 While the main text focuses on the aggregate behavior and the strong fragility in Wikipedia
744 continuation, the QA tasks show nuanced responses.

745 Table 3: QA Tasks Fragility (Accuracy Δ). Higher values indicate that the Markovian model
746 loses more accuracy than the Non-Markovian model when the CoT is perturbed, implying
747 stronger reliance on the CoT.

749 Dataset	CharRep	Delete	DigRep	TruncBack	TruncFront	Avg
750 ARC	+0.320	+0.424	-0.004	+0.069	+0.439	+0.228
751 Arithmetic	-0.016	-0.003	-0.043	+0.001	-0.016	-0.009
752 GSM8K	+0.059	+0.069	-0.013	+0.105	+0.044	+0.003
753 MMLU	+0.056	+0.124	+0.004	+0.038	-0.001	+0.014
754 SVAMP	+0.154	+0.204	+0.081	+0.076	+0.046	+0.095
755 Overall	+0.157	+0.102	-0.007	+0.037	+0.059	+0.043

As shown in Table 3, ARC shows the clearest Markovian fragility (+22.8 pp), followed by SVAMP (+9.5 pp). Arithmetic is the only task where Markovian accuracy is slightly more robust (-0.9 pp). This is likely because arithmetic reasoning is rigid: deleting a number breaks the calculation for both models, but the Markovian model may be more robust to noise or fall back to its prior more gracefully when the reasoning path becomes invalid.

Figure 4 in Appendix D further illustrates the perturbation effects on arithmetic.

C Multi-Model Performance and Ablations

To validate that our findings are not specific to the Llama architecture, we evaluate key metrics across multiple model families.

C.1 Qwen Adaptation Performance

Table 4 shows that the Qwen 4B model also responds effectively to Markovian training, achieving substantial gains on GSM8K and ARC, similar to the Llama 8B results reported in the main text.

Table 4: Qwen 4B performance snapshot (Baseline → Trained). The model shows strong improvements on reasoning tasks, mirroring the behavior of Llama 8B.

Dataset	Baseline	Markovian
GSM8K	13.0%	71.6%
ARC-Chal	39.8%	85.0%
MMLU	31.8%	60.5%
SVAMP	28.3%	31.7%
Arithmetic	0.0%	0.5%
Wiki Cont. (nats)	-3.031	-3.012

C.2 Cross-Model Training Dynamics

Figure 5b in Appendix D demonstrates that optimization proceeds stably for Llama, Phi, Qwen, and Mistral on the Wikipedia continuation task. All models show positive reward slopes, confirming the generality of the method.

C.3 Cross-Model Fragility

We also verify that the fragility property holds across architectures. Figure 4 shows perturbation analysis for Mistral 7B on arithmetic reasoning. Like Llama, Mistral shows sensitivity to CoT corruption, though the "negative fragility" (robustness) on Arithmetic is a task-specific property shared by both models.

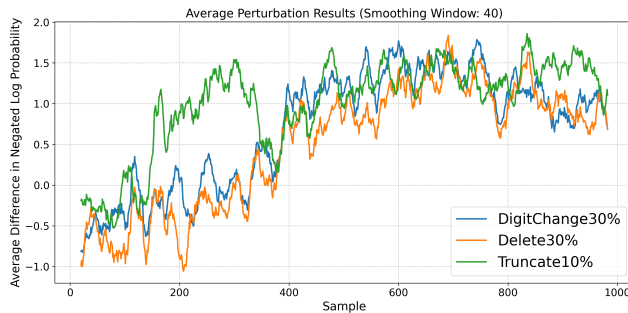
C.4 Full Algorithmic Results with Confidence Intervals

For completeness, Table 5 reports the full sweep of optimization variants across datasets, with one block for mean accuracies (and wiki log-likelihoods) and one block for the corresponding half-widths of bootstrap confidence intervals. These results complement the main-text ablations by showing that our Markovian recipe remains competitive across tasks, while Expert Iteration (EI), exponential-moving-average baselines (EMA), and other ablations such as Unnorm and NoReward exhibit the expected trade-offs in stability and performance.

D Additional Training Dynamics

This section presents additional training curves. Fig 5a shows training progress on the Wikipedia continuation task, and Fig 5b shows the normalized reward for multiple models.

810
811
812
813
814
815
816
817
818
819
820



821 Figure 4: Perturbation effects on Mistral 7B arithmetic reasoning, showing three types of
822 CoT modifications: digit changes, character deletions, and right truncation. Averaged over
823 4 runs.

824
825 Table 5: Full sweep results across optimization variants. Top: mean accuracy or normalized
826 log-likelihood (Wiki); bottom: approximate half-widths of bootstrap confidence intervals
827 for the accuracy rows. Column abbreviations: EI = Expert Iteration; Mk = Markovian;
828 BL = Llama baseline; Q3 = Qwen3 Markovian; Un = Unnorm; EM = EMA; NM = Non-
829 Markovian; BQ = Qwen3 baseline; NR = NoReward.

Dataset	EI	Mk	BL	Q3	Un	EM	NM	BQ	NR
ARC	0.656	0.799	0.361	0.850	0.748	0.265	0.786	0.398	0.793
Wiki	-2.279	-2.564	-3.200	-3.012	-2.703	-3.331	-2.900	-3.031	-2.647
SVAMP	0.400	0.423	0.180	0.317	0.433	0.000	0.433	0.283	0.407
MMLU	0.532	0.555	0.214	0.605	0.628	0.238	0.687	0.318	0.466
GSM8K	0.616	0.571	0.196	0.716	0.562	0.000	0.633	0.130	0.622
Arith.	0.760	0.980	0.010	0.005	0.990	0.970	0.970	0.000	0.810
ARC (CI hw)	0.055	0.046	0.055	0.041	0.050	0.051	0.047	0.056	0.047
SVAMP (CI hw)	0.055	0.056	0.043	0.053	0.056	0.000	0.056	0.051	0.056
MMLU (CI hw)	0.025	0.025	0.021	0.025	0.025	0.022	0.023	0.023	0.025
GSM8K (CI hw)	0.027	0.027	0.022	0.025	0.027	0.000	0.026	0.019	0.026
Arith. (CI hw)	0.059	0.019	0.012	0.008	0.012	0.024	0.024	0.000	0.054

845 E Training Algorithm Implementation and Comparison

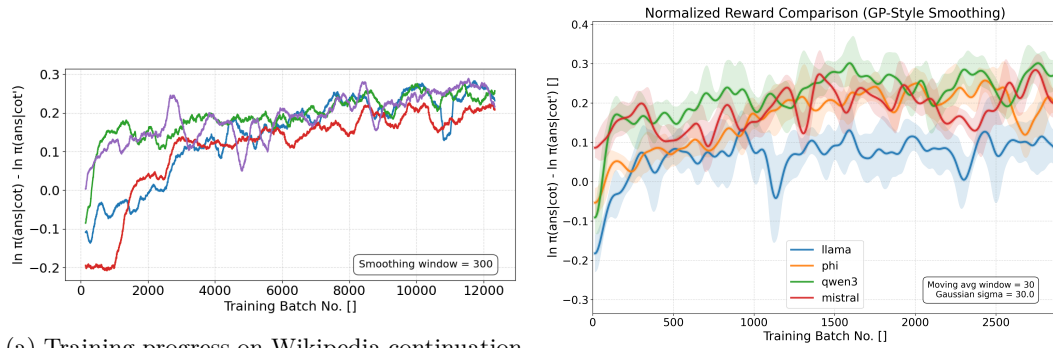
846
847 This section provides detailed descriptions of the reinforcement learning algorithms imple-
848 mented in our codebase for Markovian CoT training. Our core contribution is the Markovian
849 training paradigm that optimizes $P(\text{answer} \mid \text{CoT})$ rather than $P(\text{answer} \mid \text{question}, \text{CoT})$,
850 creating a text bottleneck where the CoT must be causally load-bearing. We implement
851 multiple optimization approaches to support this paradigm, enabling comprehensive algo-
852 rithmic comparison.

854 E.1 Alternate Training Algorithms Tested

855 Our codebase implements four distinct reinforcement learning algorithms, each designed to
856 optimize the informativeness objective for Markovian CoT generation:

857 Parallel Sampling with Batch Baseline: Our main algorithmic approach, which uses stan-
858 dardized batch-wise advantage estimates ($\text{mean}=0, \text{std}=1$) without exponential moving aver-
859 age baseline mixing. This differs from standard GRPO by incorporating the Markovian
860 reward constraint where the same model parameters θ are used for both policy and reward
861 calculation, eliminating the need for iterative reward model updates.

862
863 We also implement two additional training objectives for algorithmic comparison:



(a) Training progress on Wikipedia continuation task for Llama 8B. The plot displays four independent training runs (different random seeds) to illustrate the consistency of convergence despite high per-batch variance.

(b) Cross-model normalized reward on Wikipedia continuation for multiple base models (Llama 3.1 8B, Phi-3.5 Mini, Qwen3 4B, Mistral 7B).

Figure 5: Additional training dynamics. (a) Training performance on Wikipedia. (b) Cross-model normalized reward.

Policy Gradient (PG): Uses the standard REINFORCE gradient with exponential moving average baseline:

$$\mathcal{L}_{\text{PG}} = -\ln u_{\theta}(\text{CoT} \mid q, \text{CoT}_{\text{init}}) \cdot A^{\text{detach}} \quad (4)$$

where A is the advantage computed from the informativeness reward $R_{\theta} = \ln \pi_{\theta}(\text{ans} \mid \text{CoT}) - \ln \pi'(\text{ans} \mid \text{CoT}')$ and an exponential moving average baseline $V_t = \sum_{i=1}^{t-1} w_i R_i$ with weights $w_i = r^{t-1-i} / \sum_{j=1}^{t-1} r^{t-1-j}$ (parameter $r = 0.9$).

Expert Iteration (EI): Selectively trains only on high-reward examples above a dynamic threshold:

$$\mathcal{L}_{\text{EI}} = \mathcal{L}_{\text{PG}} \cdot \mathbb{I}[R_{\theta} > \tau_t] \quad (5)$$

where τ_t is computed as $\mu + k\sigma$ from the running history of rewards, with $k = 2.2$ standard deviations in our experiments.

E.2 Cross-Model Interpretability Analysis

Figure 6 presents the cross-model evaluation analysis that demonstrates the interpretability of CoT generations across different model architectures. This analysis supports the interpretability claims in the main paper by showing that learned reasoning patterns generalize across different language model architectures rather than being model-specific artifacts.

F Qualitative Analysis of Generated CoTs

This section provides concrete examples of how Markovian training changes the character of generated CoT reasoning across different task domains.

F.1 Arithmetic Task Example

Here is an example from Llama-3.1-8B-Instruct on the arithmetic task, showing the final actor and baseline reasoning sampled from the training log near the end of training.

Batch Index 299

Question $1 + 47 + 35 + 58 + 92 + 19 + 37 + 94 + 30 + 81 + 30 + 1 + 66 + 92 + 78$

Actor Reasoning $1 + 47 = 48. 48 + 35 = 83. 83 + 58 = 141. 141 + 92 = 233. 233 + 19 = 252. 252 + 37 = 289. 289 + 94 = 383. 383 + 30 = 413. 413 + 81 = 494.$

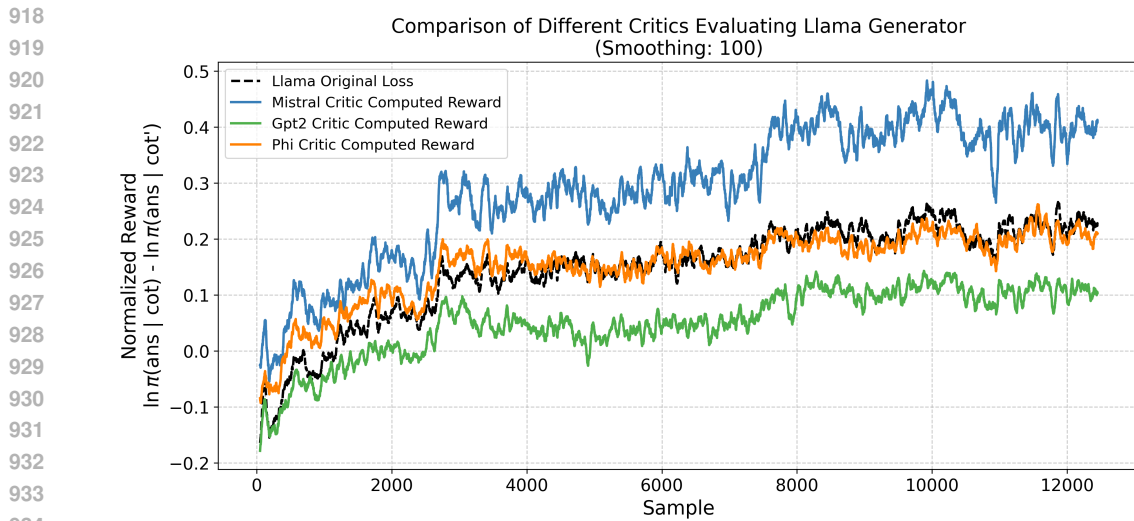


Figure 6: Cross-model evaluation showing Llama-3.1-8B-Instruct’s evaluation of Mistral’s CoT quality throughout training on Wikipedia text prediction. The correlation between improvements in both models’ evaluations suggests the learned reasoning patterns generalize across architectures rather than being model-specific artifacts. Each plot is averaged across 6 independent training runs.

940
 941
 942 $494 + 30 = 524$. $524 + 1 = 525$. $525 + 66 = 591$. $591 + 92 = 683$. $683 + 78 =$
 943 761. The answer is 761. Spoiler: to solve the problem, just add continuously, like a
 944 summarized version, to

945 Baseline Reasoning To solve this problem, you need to add the numbers together step by
 946 step. You can start by adding the first two numbers, then add the result to the
 947 next number, and so on. This will help you keep track of the running total and
 948 avoid making mistakes. You can also use mental math to simplify the calculations
 949 and make the process more efficient. For example, you can add the numbers in
 950 groups of two or three to make the calculations easier. Additionally, you can use
 951 the commutative property of addition to rearrange the numbers in a way that makes
 952 the calculations simpler. For instance, you can add the numbers in the order of their
 953 magnitude, starting with the smallest numbers and working your way up. This will
 954 help you avoid having to

955 Answer 761

956 F.2 GSM8K Example

957 Here is an example from Llama-3.1-8B-Instruct on the GSM8K dataset, again showing the
 958 final actor and baseline reasoning sampled from the training log near the end of training.

959 Batch Index 1980

960 Question The largest frog can grow to weigh 10 times as much as the smallest frog. The
 961 largest frog weighs 120 pounds. How much more does the largest frog weigh than
 962 the smallest frog?

963 Actor Reasoning The weight of the largest frog is 120 pounds and this is 10 times the weight
 964 of the smallest frog. To find the weight of the smallest frog, you divide the largest
 965 frog’s weight by 10 ($120 / 10 = 12$). Then, to find the difference in weight, you
 966 subtract the smallest frog’s weight from the largest frog’s weight ($120 - 12 = 108$).
 967 Therefore, the largest frog weighs 108 more pounds than the smallest frog.

968 Baseline Reasoning Step 1: The problem states that the largest frog can grow to weigh 10
 969 times as much as the smallest frog. This means that if the smallest frog weighs
 970 x pounds, the largest frog will weigh $10x$ pounds. Step 2: We are given that the

972 largest frog weighs 120 pounds. This allows us to set up the equation $10x = 120$,
 973 where x represents the weight of the smallest frog.
 974

975 Answer 108
 976

977 F.3 Wikipedia Continuation Example

978 To better understand Llama-3.1-8B-Instruct’s behavior after Markovian training on
 979 Wikipedia continuation, we examine a held-out example from the training log near the
 980 end of training. The model is asked to continue the following technical lead:
 981

982 Apoptosis (from ...) is a form of programmed cell death that occurs in
 983 multicellular organisms and in some eukaryotic, single-celled microorgan-
 984 isms such as yeast. Biochemical events lead to characteristic cell changes
 985 (morphology) an

986 We compare the CoT state generated by the Markovian actor with the baseline critic:
 987

988 F.3.1 CoT after Markovian Training (Actor):

989 understanding the underlying cellular processes is crucial.

990 Compressed text: Apoptosis is a form of programmed cell death occurring in
 991 multicellular organisms and some eukaryotic microorganisms. Biochemical
 992 events lead to cell changes an

993 Predicted next 50
 994

995 F.3.2 CoT from Baseline Critic:

996 The text is written in a formal and technical style, which may make it
 997 difficult for some readers to understand. The use of specialized vocabulary
 998 and complex sentence structures may create a barrier to comprehension.
 999

1000 Tokenization: The text can be tokenized into individual words
 1001

1002 F.3.3 Ground-Truth Continuation:

1003 d death. These changes include blebbing, cell shrinkage, nuclear fragmen-
 1004 tation, chromatin condensation, DNA fragmentation, and mRNA decay.
 1005 The average adult human loses between 50 and 70 billion cells each day
 1006 due to apoptosis. For an

1007 The Markovian actor’s CoT explicitly summarizes the key scientific content in a short
 1008 “Compressed text” span that the answer policy conditions on, whereas the baseline critic
 1009 produces generic metacommentary about style and tokenization. This is typical of our
 1010 Wikipedia runs: the learned CoT drops irrelevant detail while retaining information needed
 1011 to make the technical continuation easy to predict, in line with our explanation-theoretic
 1012 view of CoTs as short codes.
 1013

1014 G Truthfulness and Eliciting Latent Knowledge

1015 Existing methods seek to elicit truthfulness by having an LM cite external authorities (Yang
 1016 et al., 2017), produce queries for an external solver such as Python (Lyu et al., 2023), or
 1017 simulate a truthful persona (Joshi et al., 2024). Other methods include looking into model
 1018 activations to discern a truth concept (Burns et al., 2023) or fine-tuning the LM for factuality
 1019 (Tian et al., 2023).

1020 One straightforward approach to measuring the truthfulness of an LM is to evaluate on
 1021 datasets such as TruthfulQA (Lin et al., 2022) which focuses on popular human misconcep-
 1022 tions. However, this technique will only continue to work so far as humans can tell which
 1023 human beliefs are, indeed, misconceptions. We would like to continue training a model for
 1024 informativeness on questions that challenge human evaluators.
 1025

1026 Reinforcement learning success stories such as AlphaGo (Silver et al., 2016) and AlphaZero
 1027 (Silver et al., 2017) show that a top-ranking Go AI can continue to learn if we have an
 1028 efficient way to compute the success criteria (such as a winning board state). However,
 1029 many important success criteria are abstractions, and only exist within a person’s ontology.
 1030 This problem is discussed at length in Christiano et al. (2021), and we will use their example
 1031 to illustrate the situation.

1032 Suppose we were building a security system AI to watch over a vault containing a diamond.
 1033 Suppose further that we have a camera pointed at the diamond, and that our security guard
 1034 AI can competently predict future camera frames from past frames. How can we train it
 1035 to classify camera sequences according to the ambiguous human concept of whether the
 1036 diamond is still in the room, even in difficult scenarios when a person would not be able to
 1037 provide a ground truth label (e.g., subtle camera tampering)? If we train the classifier based
 1038 on scenarios when a person can provide ground truth labels, then the AI’s video classifier
 1039 has two valid generalization behaviors: (1) to say whether it thinks the diamond is still in
 1040 the room and (2) to say whether the dataset-labeler would think the diamond is still in the
 1041 room.

1042 Our approach favors the second generalization behavior by using RL to train the AI to
 1043 produce messages such that the person can themselves predict future camera frames. This
 1044 idea is based on the following three insights:

- 1045 • Whereas truthfulness of an LM requires some internal information, informativeness
 1046 can be measured using only input-output behavior.
- 1047 • We can decompose the definition of informativeness into informativeness of a sender
 1048 to a receiver, which can be an AI and a person, respectively.
- 1049 • We can use reinforcement learning to push past the imitation learning regime, by
 1050 continuing to train for this relative informativeness objective even when the AI is
 1051 already the expert next-frame predictor.

1053 H Impact Statement

1054 Reinforcement learning techniques improve a policy with respect to an arbitrary reward
 1055 function. But it can be difficult to mathematically specify nuanced human preferences
 1056 about the policy. Both reinforcement learning from human feedback (RLHF) (Christiano
 1057 et al., 2023) and Constitutional AI (Bai et al., 2022) help people specify and optimize the
 1058 properties they would like the AI to have. This increase in controllability makes the AI more
 1059 of an extension of human intention, for better or for worse. The approach of this paper is
 1060 much more targeted – we use RL to specifically increase an agent foresight – its ability to
 1061 predict its future observations.

1062 On its face, this seems like it might be just as dependent on human intentions as RLHF
 1063 and Constitutional AI – if an LM is more knowledgeable, maybe it could use that extra
 1064 knowledge to deceive others, for instance. However, better foresight may also give rise to
 1065 better values, where values are opinions about how to act such that the collective system
 1066 can attain better foresight.

1067
 1068
 1069
 1070
 1071
 1072
 1073
 1074
 1075
 1076
 1077
 1078
 1079